**International Journal of Emerging Engineering and Technology (IJEET)**
ISSN (e): 2958-3764
Volume: 4, Number: 2, Pages: 10 - 14, Year: 2025

# Finite Element Analysis of the Surface Mounted Permanent Motor Without Stator Excitation

Qurban Ali Shah Syed[1,*], Zahid Muhammad[2], and Kamran Ahmed Samo[3]

[1,3] Department of Electrical Engineering, The University of Larkano, Larkana, 77150, Pakistan
[2] Department of Electrical Engineering, Isra University, Hyderabad, 71000, Pakistan
[*] Corresponding author: Qurban Ali Shah Syed (Email: qurban.syed@uolrk.edu.pk)

**Received: 11/07/2025, Revised: 19/10/2025, Accepted: 10/11/2025**

***Abstract*—This paper presents an electromagnetic analysis of the brushless DC (BLDC) surface-mounted permanent magnet (SPM) motor using 2D finite element analysis (FEA). The no-load characteristics of the three-phase BLDC SPM motor are numerically computed, and the results are analysed in detail. The back EMF waveform of the three-phase BLDC SPM motor is computed when stator windings are not supplied with current, and its harmonic analysis is carried out using the fast Fourier transform (FFT). The cogging torque is computed without stator current excitation. The no-load electromagnetic results are discussed to analyse their influence on the performance of the three-phase BLDC SPM motor.**

***Index Terms*— BLDC motor, electrical machines, electro-mechanical conversion, finite element analysis, no-load analysis, permanent magnet (PM), SPM motor.**

## I. Introduction

Recently, the permanent magnet synchronous motors (PMSMs) are becoming a dominant solution to the modern electric drive applications [1], because of their high efficiency and power density, and excellent dynamic performances [2]. Among different PMSM configurations, surface-mounted permanent magnet (SPM) motors have gained significant attention for applications such as electric vehicles (EVs), aerospace actuators, industrial automation, and renewable energy systems [1]-[2]. The popularity of the SPM motors is attributed to their simple rotor structure, reduced manufacturing complexity, and reliable electromagnetic behaviour [3].

In an SPM motor, the permanent magnets (PMs) are mounted directly on the rotor surface, resulting in a nearly uniform air-gap magnetic field [4]. The SPM structure produces a predominantly sinusoidal back electromotive force (EMF) and minimises magnetic saliency [4]. Therefore, the SPM motors have almost equal direct and quadrature ($d$ and $q$) axis inductances. Hence, the control strategies are simpler, and field-oriented control (FOC) proved suitable across a wide range of operating conditions for the SPM motor [5].

The overall electromagnetic performance of the SPM motor is heavily influenced by the no-load characteristics. Under no-load conditions, the air-gap magnetic field is generated solely by the mounted PMs of the SPM motor. Therefore, the intrinsic magnetic properties of the SPM motor are investigated and have no influence on the armature reaction [6]. Thus, the no-load characteristic analysis of the SPM motor is a fundamental step in realising and optimising its electromagnetic design.

Key no-load electromagnetic characteristics of SPM motors include the air-gap magnetic flux density distribution, magnetic flux linkage, back-EMF, cogging torque, and iron losses. These parameters directly affect the SPM motor's efficiency, acoustic noise, vibration, and overall drive performance [7]. The deviations from the ideal sinusoidal air-gap magnetic field result in harmonic components in the back-EMF, which contribute to torque ripples and increased losses during operation [8].

The SPM motor inherently exposes the PMs to the airgap. Therefore, the no-load magnetic field distribution is sensitive to the magnet shape, magnetisation pattern, and the airgap geometry [4]. The stator teeth introduce spatial harmonics in the airgap flux density, due to the slotting effect. These spatial harmonics are the primary source of cogging torque even under no-load operating conditions of the SPM motor [6], [9].

Cogging torque is a parasitic effect and an important no-load characteristic in SPM motors, especially at lower speeds and for precise applications. The cogging torque arises from the interaction of the rotor PMs and the stator slotting; therefore, the periodic variations in magnetic reluctance are developed [9]. Excessive cogging torque causes the speed oscillations, acoustic noise, and degraded control performance of the SPM motor [5], [9]. Therefore, accurate prediction and mitigation of cogging torque are important for high-performance SPM motor applications.

Another important aspect of the SPM motor's no-load behaviour is its back-EMF characteristic. The back EMF reflects the airgap magnetic flux distribution and winding configuration [10]. The amplitude and harmonic content of the

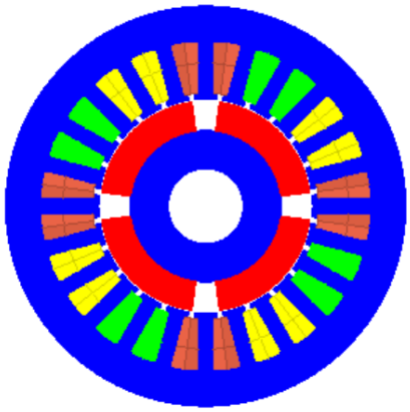

**Fig. 1.** Three-phase BLDC SPM motor.

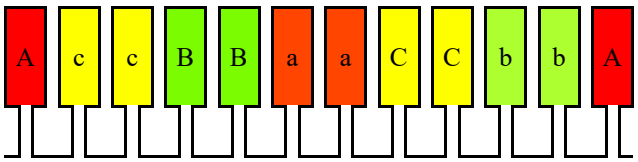


**Fig. 2.** Three-phase base-winding scheme for the BLDC SPM motor.

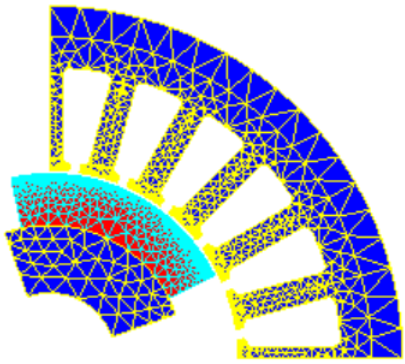

**Fig. 3.** Meshing of the BLDC SPM motor.

back-EMF determine the voltage utilisation, the maximum achievable speed, and the inverter requirements for the SPM motor application [11]. Thus, the sinusoidal back-EMF under no-load conditions is often a primary design objective for the SPM motor, ensuring smooth electromagnetic torque production under load [4].

The iron losses under no-load conditions are quite significant for overall efficiency considerations in SPM motors, especially at high rotational speeds [12]. The no-load iron losses are mainly composed of the hysteresis and eddy current losses in the stator and rotor core of the SPM motor. The no-load iron losses provide a valuable insight for the magnetic material selection and magnetic flux density saturation within the SPM motor [12]. Accurate estimation of the iron losses is crucial for the thermal design and efficiency optimization of the SPM motors.

Analytical methods, the finite element analysis (FEA) numerical method, and experimental measurement setups are commonly employed to evaluate the no-load electromagnetic characteristics of SPM motors [4]. While the analytical models offer physical insight and rapid evaluation, the FEA method enables the detailed investigation of the complex geometries, nonlinear magnetic behaviour, and slotting effects of the SPM motor [13]. Despite this, experimental validation remains indispensable for verifying the accuracy of theoretical and numerical predictions [13-16].

This paper presents a comprehensive investigation of the no-load electromagnetic characteristics of brushless DC (BLDC) SPM motors. The detailed analysis of the no-load electromagnetic behaviour of the BLDC SPM motor highlights the airgap magnetic flux distribution, the back-EMF, and the cogging torque.

## II. BLDC SPM Motor

The BLDC SPM motor is characterised by specific geometric and physical dimensions, designed for pump applications. The BLDC SPM motor comprises the fixed part, the stator, and the movable part, the rotor, separated by an air gap, as shown in Fig. 1. The stator of the BLDC SPM motor includes the yoke, slots, and three-phase stator windings, while the rotor iron of the motor holds the surface-mounted PMs.

Key physical characteristics of the BLDC SPM motor include 24 stator slots, a 3-phase Y-connection, and 2 pole pairs, as shown in Fig. 1. The three-phase BLDC SPM motor utilises the NdFeB magnets mounted on the rotor. Whereas, the stator of the BLDC SPM motor's winding is a 3-phase concentric type winding having a throw of 5 coils, and a coil per pole per phase, as shown in Fig. 2.

The three-phase BLDC SPM motor's outer diameter is 48 mm, and its stack length is 50.308 mm for the pump application. The airgap length is 0.503 mm. The rotor's shaft radius is 9.003 mm, and the rotor's external radius is 25.154 mm. The PMs are mounted on the rotor and have a thickness of 6.987 mm with a PM pole arc of 150°. The stator slots are square-shaped with a radial depth of 14 mm, slot opening of 1.5 mm and the tooth width of 3.4 mm.

## III. Methodology

The simulation of back electromotive force (EMF) for the BLDC SPM motor involves a specific methodology within the Flux software [14]. This process is designed to compute the back EMF when the BLDC SPM motor operates as a generator. The computation is performed at no load, and the BLDC SPM motor is running at a speed of 1000 rpm. The first step for the electromagnetic simulation is to create the geometry of the BLDC SPM motor.

Next step is to mesh the geometry of the BLDC SPM motor. The line meshing is performed, and specifically fine meshing is imposed at the lines facing the airgap, as shown in Fig. 3. The PM's and stator tooth towards the airgap are finely meshed, as shown in Fig. 3. The airgap length is divided into two parts, one

rotating and another stator airgap for the proper interaction of the rotor and stator of the BLDC SPM motor [17-18].

The physical application of a transient magnetic 2D application is selected for the no-load electromagnetic characteristic computation of the BLDC SPM motor. The transient initialization is set with a zero initial solution. The materials are defined especially two materials, i.e., electrical steel and magnet. The stacked laminated electrical steel is selected for the stator and rotor core, similarly, the PM material is described by its remanent flux density of 1.12 T and a relative permeability of 1.1.

Two mechanical sets are defined to differentiate the fixed and moving parts of the rotatory three phase BLDC SPM motor. The rotor rotates at a constant speed of 1000 rpm, whereas the stator is fixed. An electrical circuit is defined, consisting of the coils and inductances corresponding to the stator coils with their respective winding scheme. No current is supplied to the stator coils, therefore, the BLDC SPM motor runs as a generator. As the BLDC SPM motor's no-load characteristics are computed, the stator phase resistances have a large value for the back EMF computation.

The face regions are modified and assigned to accurately describe their respective physical properties. The coil conductor regions are defined by specified components, turns, and orientations, without a current supply. The ferromagnetic face regions are defined with their respective materials and mechanical sets. The PM orientation for the magnet face region is defined, and the face regions are assigned to the respective rotatory mechanical set. After defining the physics, a solving scenario is created, and the rotor's rotation is controlled by time from 0 to 0.03 sec.

## IV. No-Load Characteristics

The three-phase BLDC SPM motor has a magnetic field generated by the PMs, and it is not excited by the stator winding for the no-load electromagnetic characteristic analysis. Thus, the magnetic flux density is solely due to the PMs and is shown in Fig. 4. The stator as well as rotor cores of the BLDC SPM motor are of laminated electrical steel, whereas the stator coils are not supplied with current. Although PM's residual magnetic flux density is 1.12 T, the magnetic flux density in the electrical steel reaches to 2.2 T, especially in the stator tooth due to the electrical steel's higher magnetic flux saturation level and permeance.

Without stator current excitation, the back EMF for the three-phase BLDC SPM motor yields a waveform, as shown in Fig. 5. The three-phase induced voltage of the BLDC SPM motor is computed across the coil conductors as a function of the rotor's angular position. Thus, the $V_1$, $V_2$, and $V_3$ voltages of phase A, B and C of the BLDC SPM motor against time is shown in Fig. 5. The time interval for this plot ranges from 0 to 0.03 seconds. It is evident that the back EMF of the BLDC SPM motor is not purely sinusoidal; therefore, its harmonic analysis needs to be carried out.

The harmonic analysis of the back EMF involves the fast Fourier transform (FFT) of the voltage through a stranded coil,

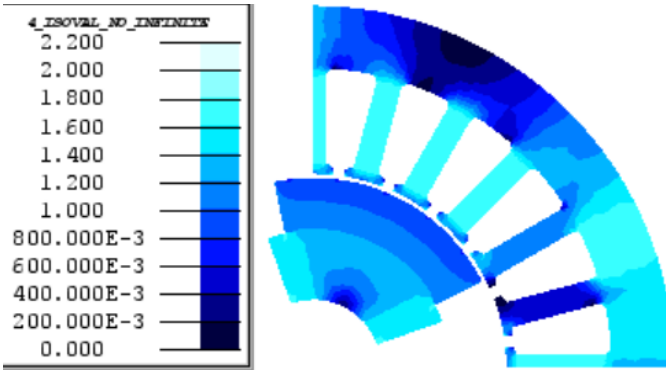


**Fig. 4.** Distribution of the magnetic flux density from 0.0 T to 2.2 T.

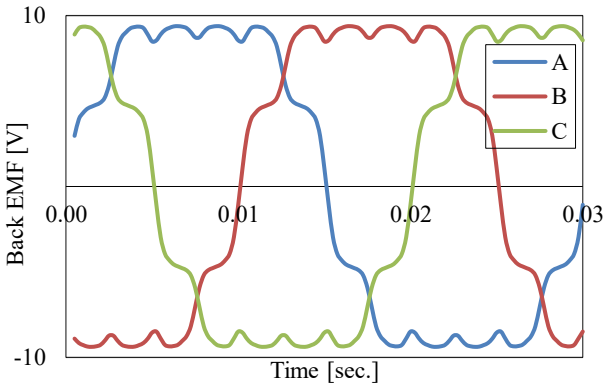


**Fig. 5.** Back EMF of the brushless SPM motor.

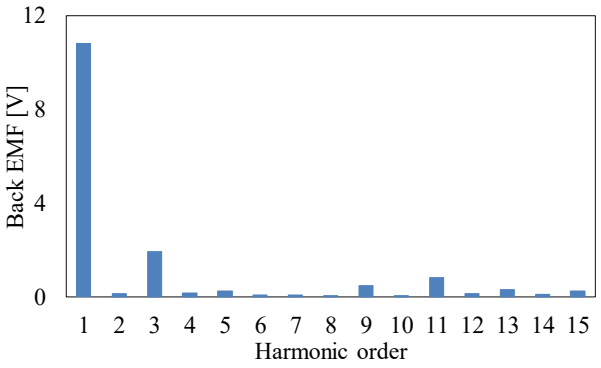


**Fig. 6.** Spectra of the back EMF of the brushless SPM motor.

as shown in Fig. 6. It is done for a full period of the back EMF of the BLDC SPM motor, analyzing the $V_1$ curve without a DC component and up to 15 harmonics. The FFT analysis of the back EMF reveals the harmonic content of the back EMF. The spatial harmonics provide an important understanding of the BLDC SPM motor's performance and potential issues like the torque ripples.

As, the magnet pole pair and 12 stator slots face each other, during a complete electrical cycle. Thus, the $11^{th}$ and $13^{th}$ harmonics appear. Although the $3^{rd}$ harmonic is more parasitic, these harmonics are significant as they contribute to the noise, vibration, and additional losses in the BLDC SPM motor. Thus,

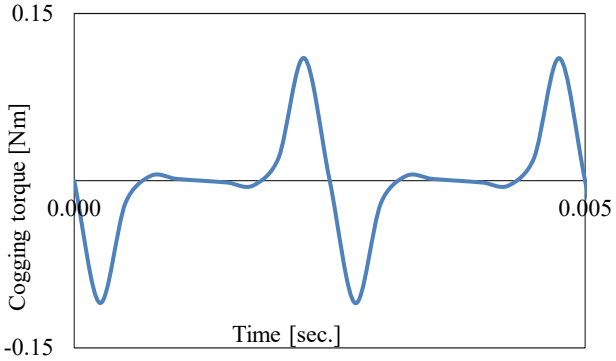


**Fig. 7.** Cogging torque of the brushless SPM motor.

the harmonic analysis refines the next design stage of the three-phase BLDC SPM motor and its control strategies.

Cogging torque is a parasitic torque that occurs in rotary electrical machines, even when no current flows through the stator windings. Thus, in the three-phase BLDC SPM motor, the cogging torque is caused by the interaction between the PMs mounted on the rotor and the stator's electrical steel teeth. The cogging torque causes undesirable effects such as vibration, noise, and difficulty in achieving smooth low-speed operation of the three phase BLDC SPM motor for the pump applications.

The cogging torque results are presented in Fig. 7, and the peak cogging torque is calculated to be 0.0119 Nm. The cogging torque of the BLDC SPM motor is a critical parameter for evaluating the motor performance and its operational smoothness. Thus, minimizing the cogging torque is an essential task for the high-performance three phase BLDC SPM motor applications.

## V. Conclusion

The back EMF is the fundamental characteristic of the BLDC SPM motor. Back EMF is induced when the rotor rotates and is magnetically excited, whereas the stator is fixed and not excited. It represents the voltage induced in the stator windings due to the changing magnetic flux from the PMs. The back EMF of the three-phase BLDC SPM motor is computed at a constant speed of 1000 rpm, and the BLDC SPM motor operates as a generator without load conditions. Back EMF is crucial to BLDC SPM motor design, as it directly influences torque-speed characteristics and overall motor performance.

Spectrum analysis of the back EMF using the FFT provides detailed insights into the harmonic content of the BLDC SPM motor's back EMF waveform. This analysis helps identify the undesirable harmonics that arise from the interaction between the PMs and the stator slots during an electrical cycle. The analysis of the spatial harmonics is important for assessing the quality of the back EMF waveform and to predict potential issues like torque ripple, noise, and additional losses in the three-phase BLDC SPM motor.

The cogging torque is an intrinsic characteristic of the BLDC SPM motor. It occurs even when the windings are not supplied with current. Thus, the cogging torque results from the magnetic attraction between the rotor's PMs and the stator's slotted structure. The airgap reluctance varies and cogging torque is developed. The peak cogging torque of 0.0119 Nm is a parasitic effect, and it leads to the BLDC SPM motor's vibrations and noise, particularly at low speeds, hence, it affects the BLDC SPM motor's smooth operation.

Thus, the back EMF, its harmonic spectrum, and cogging torque are important parameters for the characterissation and optimization of the three-phase BLDC SPM motor. The back EMF of the BLDC SPM motor defines the motor's electrical response of the magnetic flux linkage. The back EMF's spectrum analysis highlights the waveform distortions caused by the BLDC SPM motor's design specifics. Cogging torque is a mechanical ripple that directly affects the smoothness of the three-phase BLDC SPM motor's operation. The comprehensive analysis of these factors provides a fundamental basis for developing an efficient, high-performance three-phase BLDC SPM motor for pump applications.

## ACKNOWLEDEGEMENTS

Corresponding author* acknowledges the support of Altair® for the FEM license during the PhD research at the chair of Electrical Drives and Machines, FAU University of Erlangen-Nuremberg. The simulation and technical process is adopted from the Flux solver manual.

## CONFLICT OF INTEREST

The authors declare no conflicts of interest to report regarding the present study.

## AUTHOR CONTRIBUTIONS

Conceptualization, methodology, software, validation, writing—original draft preparation, Q. A. S. Syed; writing—review and editing, Q. A. S. Syed, K. A. Samo and Z. Muhmmad.

## FUNDING STATEMENT

This research received no external funding.

## INSTITUTIONAL REVIEW BOARD STATEMENT

Not applicable.

## INFORMED CONSENT STATEMENT

Not applicable.

## DATA AVAILABILITY STATEMENT

Data is available on reasonable request.

## References

[1] Nategh, Shafigh, Aldo Boglietti, Yujing Liu, Daniel Barber, Ron Brammer, David Lindberg, and Ola Aglen. "A review on different aspects of traction motor design for railway applications." *IEEE Transactions on Industry Applications* 56, no. 3 (2020): 2148-2157.

[2] De Santiago, Juan, Hans Bernhoff, Boel Ekergård, Sandra Eriksson, Senad Ferhatovic, Rafael Waters, and Mats Leijon. "Electrical motor

drivelines in commercial all-electric vehicles: A review." *IEEE Transactions on vehicular technology* 61, no. 2 (2011): 475-484.

[3] C. Liu, K. T. Chau, C. H. T. Lee and Z. Song, "A Critical Review of Advanced Electric Machines and Control Strategies for Electric Vehicles," in *Proceedings of the IEEE*, vol. 109, no. 6, pp. 1004-1028, June 2021.

[4] S. Q. A. Shah, T. A. Lipo and B. -I. Kwon, "Modeling of Novel Permanent Magnet Pole Shape SPM Motor for Reducing Torque Pulsation," in *IEEE Transactions on Magnetics*, vol. 48, no. 11, pp. 4626-4629, Nov. 2012, doi: 10.1109/TMAG.2012.2197188.

[5] K. Matsuse and D. Matsuhashi, "New technical trends on adjustable speed AC motor drives," in *Chinese Journal of Electrical Engineering*, vol. 3, no. 1, pp. 1-9, 2017.

[6] Q. A. S. Syed and I. Hahn, "Analysis of flux focusing double stator and single rotor axial flux permanent magnet motor," *2016 IEEE International Conference on Power Electronics, Drives and Energy Systems (PEDES)*, Trivandrum, India, 2016, pp. 1-5, doi: 10.1109/PEDES.2016.7914324.

[7] Q. A. S. Syed and I. Hahn, "Influence of the Magnetic Bridges on the Flux Focusing Type Axial Flux Permanent Magnet Motor," *2018 IEEE Electrical Power and Energy Conference (EPEC)*, Toronto, ON, Canada, 2018, pp. 1-6, doi: 10.1109/EPEC.2018.8598318.

[8] D. G. Dorrell, M. -F. Hsieh, M. Popescu, L. Evans, D. A. Staton and V. Grout, "A Review of the Design Issues and Techniques for Radial-Flux Brushless Surface and Internal Rare-Earth Permanent-Magnet Motors," in *IEEE Transactions on Industrial Electronics*, vol. 58, no. 9, pp. 3741-3757, Sept. 2011.

[9] Abid, Muhammad Haseeb, Wasif Shafiq, Muhammad Dayem, and Hassan Riaz Khan. "Step-by-Step Installation of Solar Energy and Its Maintenance." *International Journal of Emerging Engineering and Technology* 4, no. 1 (2025): 1-5.

[10] Islam, Abdullah, Ahmad Saeed, Adeel Hassan, and Zeeshan Shahid. "AI-Powered Home Automation: A Simple and Smart Living Solution." *International Journal of Emerging Engineering and Technology* 4, no. 1 (2025): 6-10.

[11] Q. A. S. Syed, M. A. Solangi, and M. A. Shah, "Cogging torque reduction in induction motor through rotor skewing", Sir Syed University Research Journal of Engineering & Technology, vol. 15, no. 2, 2025. https://doi.org/10.33317/ssurj.709

[12] Naseer, F., Khan, M. N., & Altalbe, A. "Intelligent time delay control of telepresence robots using novel deep reinforcement learning algorithm to interact with patients,"Applied Sciences,13(4), 2462, 2023.

[13] Jamil, M., Khan, M. N., Rind, S. J., Awais, Q., & Uzair, M. "Neural network predictive control of vibrations in tall structure: An experimental controlled vision,"Computers & Electrical Engineering,89, 106940, 2021.

[14] K. -T. Kim, J. -K. Park, J. Hur and B. -W. Kim, "Comparison of the Fault Characteristics of IPM-Type and SPM-Type BLDC Motors Under Inter-Turn Fault Conditions Using Winding Function Theory," in *IEEE Transactions on Industry Applications*, vol. 50, no. 2, pp. 986-994, March-April 2014.

[15] Q. Han, N. Samoylenko and J. Jatskevich, "Average-Value Modeling of Brushless DC Motors With 120° Voltage Source Inverter," in *IEEE Transactions on Energy Conversion*, vol. 23, no. 2, pp. 423-432, June 2008.

[16] Q. A. S. Syed, Spoke Type Axial Flux Permanent Magnet Motor and its Flux Switching Variants, Ph.D. dissertation, Friedrich-Alexander-Universität Erlangen-Nürnberg, Technische Fakultät, 2025. DOI: 10.25593/open-fau-2172.

[17] H. -C. Liu, H. W. Kim, H. K. Jang, I. -S. Jang and J. Lee, "Ferrite PM Optimization of SPM BLDC Motor for Oil-Pump Applications According to Magnetization Direction," in *IEEE Transactions on Applied Superconductivity*, vol. 30, no. 4, pp. 1-5, June 2020.

[18] Altair Engineering, Inc. Altair Flux 2D: Finite element software for low-frequency electromagnetic and thermal simulations tutorial, 2025. [Available]: https://altair.com/flux.